

Reconstruction of Twist Torque in Main Parachute Risers

Joshua D. Day¹

Embry-Riddle Aeronautical University, Prescott, AZ, 86301

The reconstruction of twist torque in the Main Parachute Risers of the Capsule Parachute Assembly System (CPAS) has been successfully used to validate CPAS Model Memo conservative twist torque equations. Reconstruction of basic, one degree of freedom drop tests was used to create a functional process for the evaluation of more complex, rigid body simulation. The roll, pitch, and yaw of the body, the fly-out angles of the parachutes, and the relative location of the parachutes to the body are inputs to the torque simulation. The data collected by the Inertial Measurement Unit (IMU) was used to calculate the true torque. The simulation then used photogrammetric and IMU data as inputs into the Model Memo equations. The results were then compared to the true torque results to validate the Model Memo equations. The Model Memo parameters were based off of steel risers and the parameters will need to be re-evaluated for different materials. Photogrammetric data was found to be more accurate than the inertial data in accounting for the relative rotation between payload and cluster. The Model Memo equations were generally a good match and when not matching were generally conservative.

Nomenclature

<i>BET</i>	=	Best Estimate Trajectory
<i>CDT</i>	=	Cluster Development Test
<i>CM</i>	=	Center of Mass
<i>CPAS</i>	=	Capsule Parachute Assembly System
<i>EDU</i>	=	Engineering Unit Development test program
$F_{v,i}$	=	Riser force for riser <i>i</i>
<i>IMU</i>	=	Inertial Measurement Unit
<i>k</i>	=	Wind up and Wind down factor
$M_{f,i}$	=	Torque in twist formation stage for riser <i>i</i>
<i>MPCV</i>	=	Orion/Multi Purpose Crew Vehicle
<i>PCDTV</i>	=	Parachute Compartment Drop Test Vehicle
ϕ	=	Twist angle
ϕ^*	=	Point at which risers begin formed twist (178.2°)
<i>P</i>	=	Roll
<i>PTV</i>	=	Parachute Test Vehicle
$\dot{\Psi}$	=	Twist Rate
<i>Q</i>	=	Pitch
<i>R</i>	=	Yaw
<i>RCS</i>	=	Reaction Control System
R_f	=	Effective radius from fly-out centerline to contact area between the riser and fairlead
$R_{fairlead}$	=	Radius of the fairlead
R_{cable}	=	Radius of the riser
R_W	=	Radius of the risers in formed twist
θ	=	Parachute Fly-out Angle
W_V	=	Vehicle Weight

¹ Student, Embry-Riddle Aeronautical University, 3700 Willow Creek Rd., Prescott, AZ 86301, AIAA Member.

compute the fly-out angles and the twist angle. The Model Memo Torque Equation was then used again to calculate the twist torque. The values from the true torque were then compared to the two values given by the Model Memo equation to ensure a good match and validate the Model Memo Conservative Torque Equation.

II. Equations and Assumptions

There are two phases of twisting. The first phase is called the “twist formation” phase^[1]. The “twist formation” phase is characterized under low twist angles, where a torque is applied by the friction of the risers on the fairlead. As a riser is pulled against the edge of the fairlead, it causes a moment to be formed on the CM and a twist to begin forming about the fly-out axis (θ).

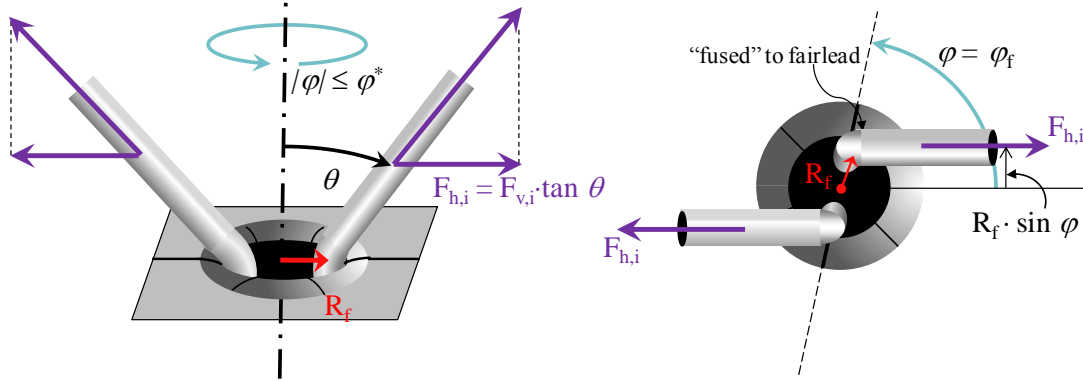


Figure 2. Twist formation (2-risers).

The torque during the twist formation stage is given by Eq. 1:

$$M_{f,i} = -R_f \cdot F_{v,i} \cdot \tan(\theta) \cdot \sin(\phi_f) \quad (1)$$

R_f is the effective radius from the centerline to the contact area between the riser and the fairlead. R_f is given by Eq. 2:

$$R_f = R_{\text{fairlead}} - R_{\text{cable}} \quad (2)$$

$F_{v,i} \cdot \tan(\theta)$ is the horizontal component of the riser force acting on the fairlead. In steady state conditions the conservative summation of riser tension vertical components equals the weight of the vehicle therefore the expression becomes Eq. 3:

$$M_f \approx -W_v \cdot \tan \theta \cdot R_f \cdot \sin \phi \quad (3)$$

The factor $\sin(\phi_f)$ accounts for the effect of the twisting rotation of the risers about the fly-out axis. Due to the fused and slipped conditions empirically found in the twist formation stage the torque curve must be stretched by multiplying the twist angle by $\frac{3}{4}$ to calculate an estimated effective fairlead twist angle. This implies that $\phi_f \approx \frac{3}{4} \phi$. Therefore, the twist formation expression becomes Eq. 4:

$$M_f \approx -R_f \cdot W_v \cdot \tan(\theta) \cdot \sin\left(\frac{3}{4} \phi\right) \quad (4)$$

The second phase is the “formed twist” phase. The formed twist phase begins after the risers rotate enough to start wrapping around each other.

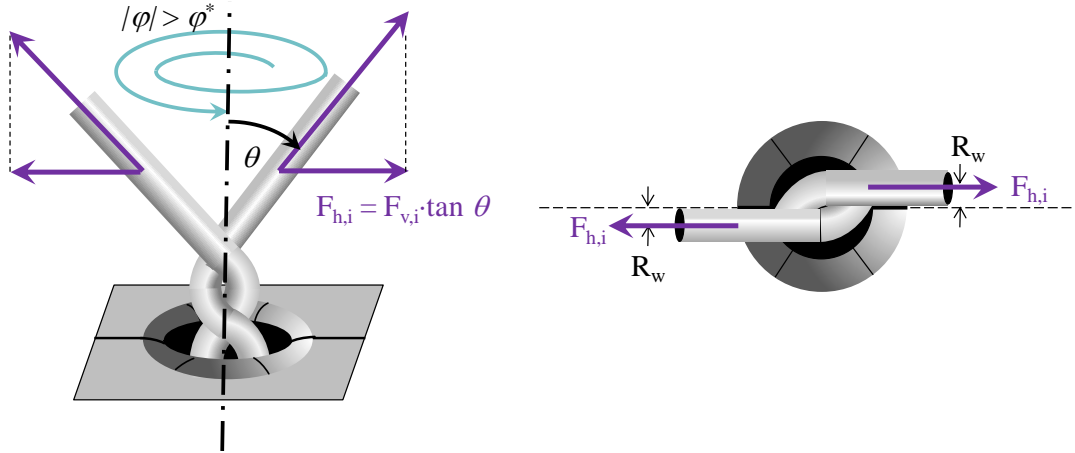


Figure 3. Formed twist diagram.

A new torque radius is developed based on the geometry of the twisted risers. The base formed twist torque is given by the expression:

$$M_f \approx -R_w \cdot W_v \cdot \tan(\theta) \quad (5)$$

The new radius that is formed, R_w , is dependent on the riser thickness and the riser geometry in the twisted phase. Based on a relationship between riser diameter and a formed twist phase theoretical radius, R_w , changes with the number of risers. This is shown below, where R , is the measured riser radius.

$$\begin{array}{ll} \text{2-Riser} & R_{w,\text{theoretical}} = R \\ \text{3-Riser} & R_{w,\text{theoretical}} = 1.15R \end{array}$$

There is a difference in torque while being wound up as opposed to being unwound. Experimental data showed that the relationship was $M_{\text{up}} \cong k \cdot M_{\text{down}}$, where $k = 1.3$. An experimental method to determine the effective radius of the twisted risers based on testing geometry was developed. This experimental radius was determined using Eq. 6 below. The experimentally determined radius, $R_{w,\text{exp}}$, had a smaller value than the theoretically calculated values, but matched ground test data better. Differences between theoretical and experimental radius values are due to the interaction between the risers. As the risers wind around each other, the steel ropes tend to flatten out.

$$R_{w,\text{exp}} = \frac{dh}{d\phi} \frac{1}{\tan(\theta_0)} \quad (6)$$

Figure 4 shows the differences in how well the experimental and theoretical radii match the test data. The experimentally determined radius (dashed black line) provides a closer match for wind-up data, while the theoretical radius provides a conservative value.

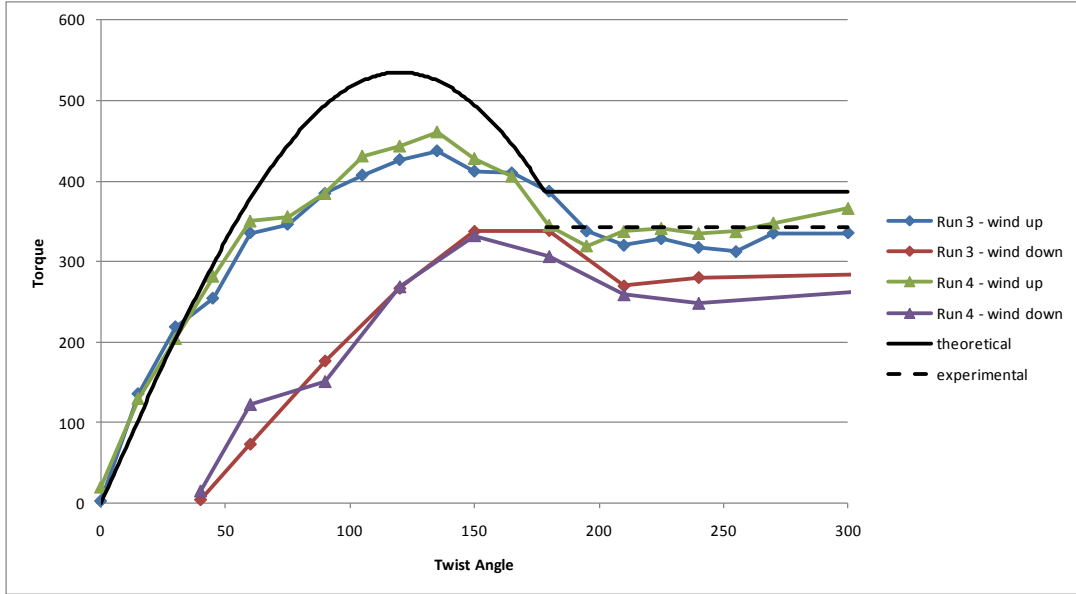


Figure 4. Conservatiave model and $\theta = 15.5^\circ$ ground test data

The conservative torque equation becomes Eq. 7:

$$M_f = \begin{cases} -R_f \cdot F_v \cdot \tan(\theta) \sin\left(\frac{3}{4}\phi\right), & \text{if } |\phi| < \phi^* \\ -k \cdot R_w \cdot F_v \cdot \tan(\theta) \cdot \text{sign}(\phi), & \text{if } |\phi| \geq \phi^* \end{cases} \quad (7)$$

Where:

$F_v \approx$ Suspended Vehicle Weight (W_v)

R_w = effective radius of the twisted risers

R_f = effective radius from the centerline to the contact area between the riser and the fairlead

$k = 1.3$ for $\dot{\phi} \geq 0$, 1.0 for $\dot{\phi} < 0$

$\phi^* = 178.2^\circ$

The twist formation phase is represented by the first part of Eq. 7 and the formed twist phase begins at ϕ^* and is defined by the second part of Eq. 7. The ϕ angle was determined by both the IMU data and photogrammetrics. Figure 5 and Eq. 8 show how photogrammetrics were used to calculate ϕ .



Figure 5. Photogrammetric ϕ angle.

$$\theta_2 - \theta_1 = \phi \quad (8)$$

Figure 6 shows the body rates P, Q, and R and the assumed twist rate ($\dot{\Psi}$) axis.

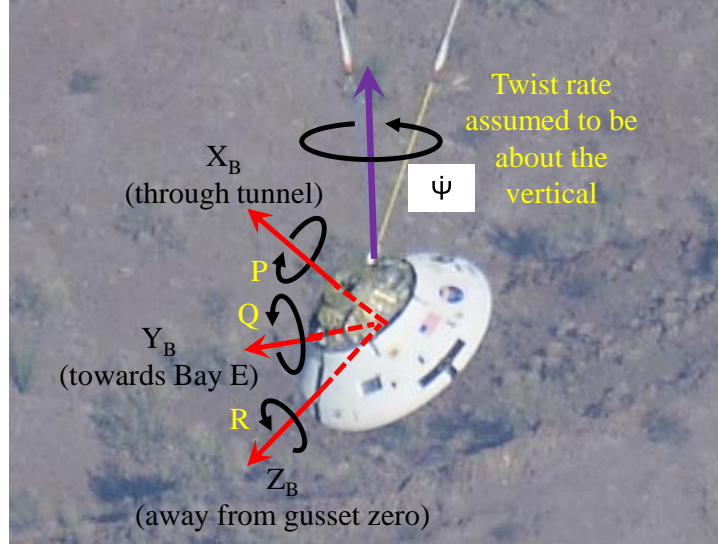


Figure 6. Twist rate compared to body rates.

The twist rate is calculated using the pitch, roll, yaw, and their rates from the IMU data as shown in the following rates transformation Eq. 9:

$$\begin{bmatrix} \dot{\phi} \\ \dot{\theta} \\ \dot{\Psi} \end{bmatrix} = \begin{bmatrix} 1 & 0 & 0 \\ 0 & \cos(roll) & -\sin(roll) \\ 0 & \sin(roll) & \cos(roll) \end{bmatrix} * \begin{bmatrix} \cos(pitch) & 0 & \sin(pitch) \\ 0 & 1 & 0 \\ -\sin(pitch) & 0 & \cos(pitch) \end{bmatrix} * \begin{bmatrix} \cos(yaw) & -\sin(yaw) & 0 \\ \sin(yaw) & \cos(yaw) & 0 \\ 0 & 0 & 1 \end{bmatrix} * \begin{bmatrix} P \\ Q \\ R \end{bmatrix} \quad (9)$$

The derivative of the twist rate is then multiplied by the inertia to calculate the true torque, such that $M_f = [\dot{\Psi}] * [I]$. The twist moments are given by the Eq. 10:

$$\begin{bmatrix} M_x \\ M_y \\ M_z \end{bmatrix} = [I] * \begin{bmatrix} \dot{P} \\ \dot{Q} \\ \dot{R} \end{bmatrix} + \left(\begin{bmatrix} P \\ Q \\ R \end{bmatrix} \times [I] * \begin{bmatrix} P \\ Q \\ R \end{bmatrix} \right) \quad (10)$$

III. Test Reconstruction

A. Phase I: CDT-2-2 Platform Test

The first test to be reconstructed was used for simplicity and to validate the reconstruction technique. The test was a platform test with 1-DOF, no confluence, and it was stable. The first step to reconstruct the twist torque was to look at video footage of the test drops and determine the times at which each phase began and ended and when there was wind up or wind down. The lack of confluence caused the R_f parameter to be zero and only the second function in the Model Memo Conservative Torque Equation: Eq. 7, to be used. The data was then run through the simulation according to Fig. 7.

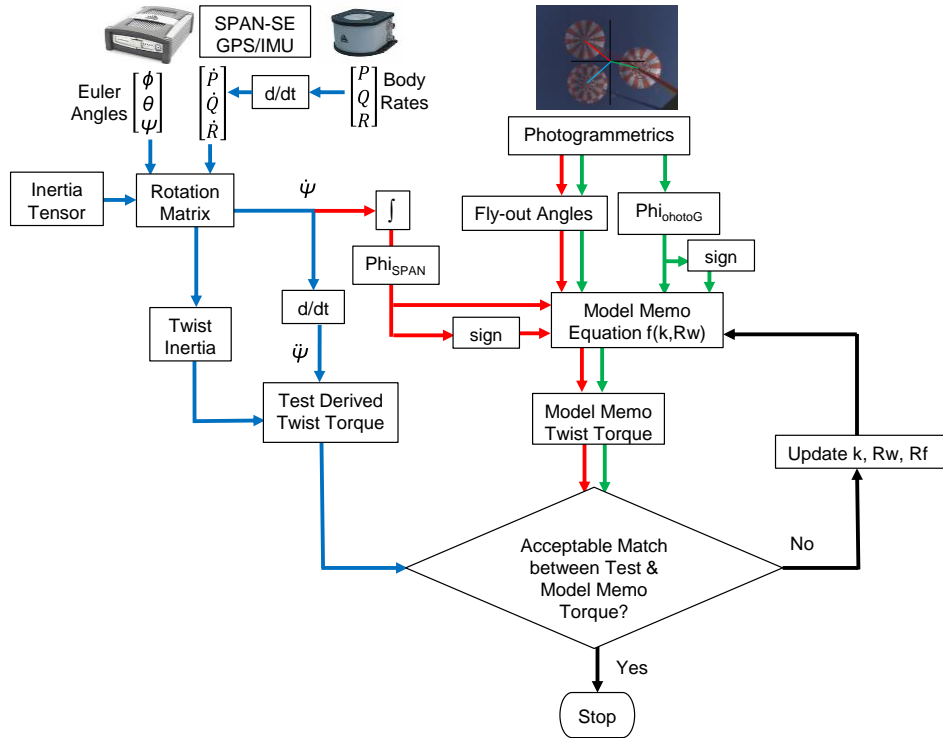


Figure 7. Simulation Methodology.

The twist angles (ϕ) from the SPAN-SE and the photogrammetrics were compared to ensure a good match. They were also adjusted to be at zero twist at the same times that the video showed zero twist. Once a good match was made the simulation was run again to calculate the twist torque.

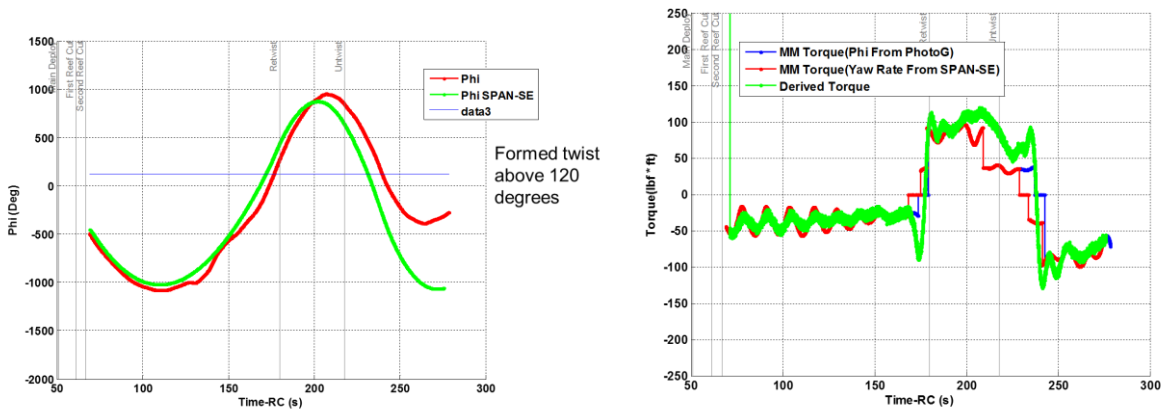


Figure 8. Twist angle and Twist Torque Reconstructions.

As Fig. 8 shows, there was a good match between the true torque or “derived torque” (in green) and the Model Memo torque equations (blue and red). It can also be seen that the Model Memo equations are indeed conservative. CDT-2-2 had only two main parachutes on a confluence, which caused the formed twist to start when the twist angle was above 120° instead of 178.2° in a fairlead. This data proved that the technique of reconstruction was viable and the Model Memo Torque Equation was accurate enough to match the true torque. This provided the rationale to continue to Phase II and begin reconstruction of EDU tests.

B. Phase II: CDT-3-1 and CDT-3-2 PCDTV Test

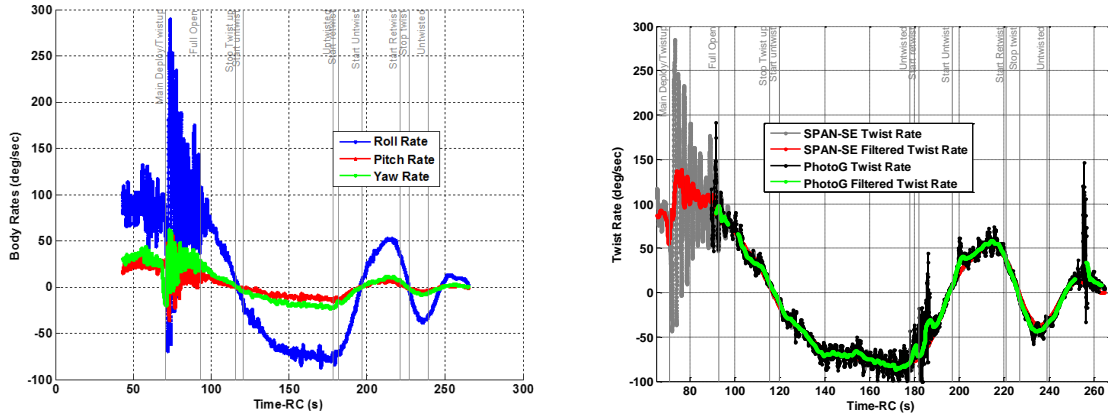


Figure 11. CDT-3-1 Body Rates and Roll/Twist Rates.

The simulation was then run to calculate the true or reconstructed twist torque (blue trace in Fig. 12) and the Model Memo twist torque (green and red traces in Fig. 12). They were a good match, and the Model Memo predicted torque proved to be conservative but follow the true torque trend very well.

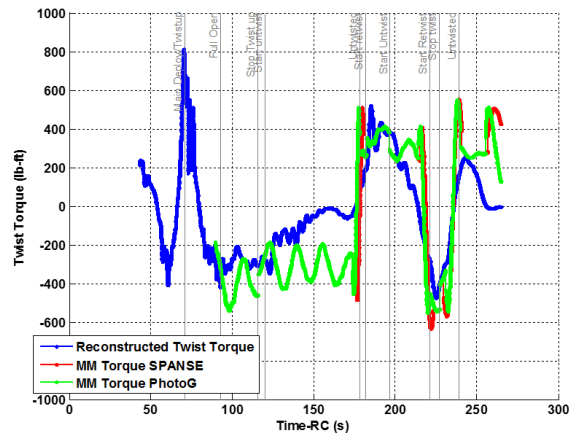


Figure 12. CDT-3-1 Twist Torque.

2. CDT-3-2

CDT-3-2 used the same method as CDT-3-1. The twist rate was again almost all created by the roll as shown by the flight test data in Fig. 13.

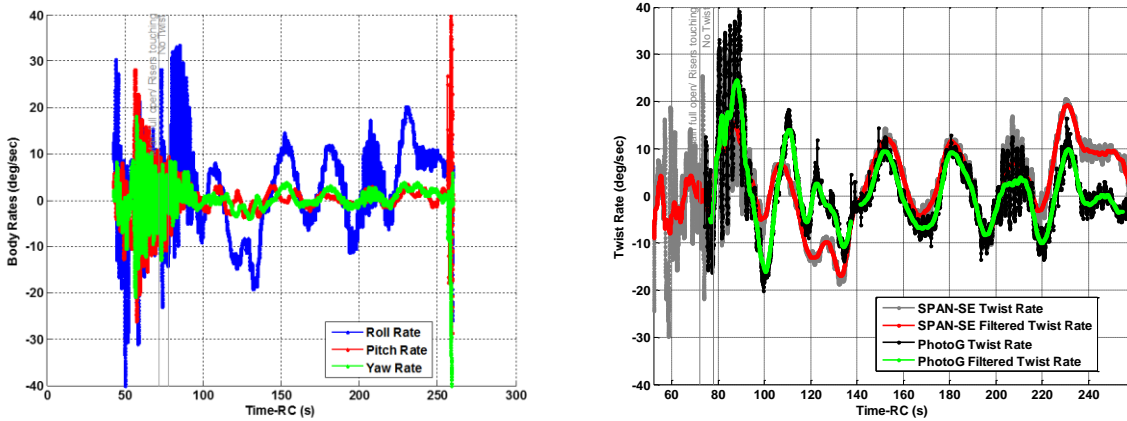


Figure 13. CDT-3-2 Body Rates and Roll/Twist Rate.

The IMU data showed a complete twist in the last minute of flight but after review of the video footage it was discovered that the parachutes and the PCDTV rotated at the same speed during that time and there was no twist. The IMU reads what the PCDTV does and does not account for the movement of the parachutes, whereas the photogrammetrics uses the relative motion of the chutes to the body. The discrepancies between the twist angle using the IMU or SPAN-SE data and the twist angle using photogrammetrics is shown in Fig. 14. The simulation was then run to calculate the twist torque. The Model Memo torque using the photogrammetric data provided a good match to the true torque and was once again conservative.

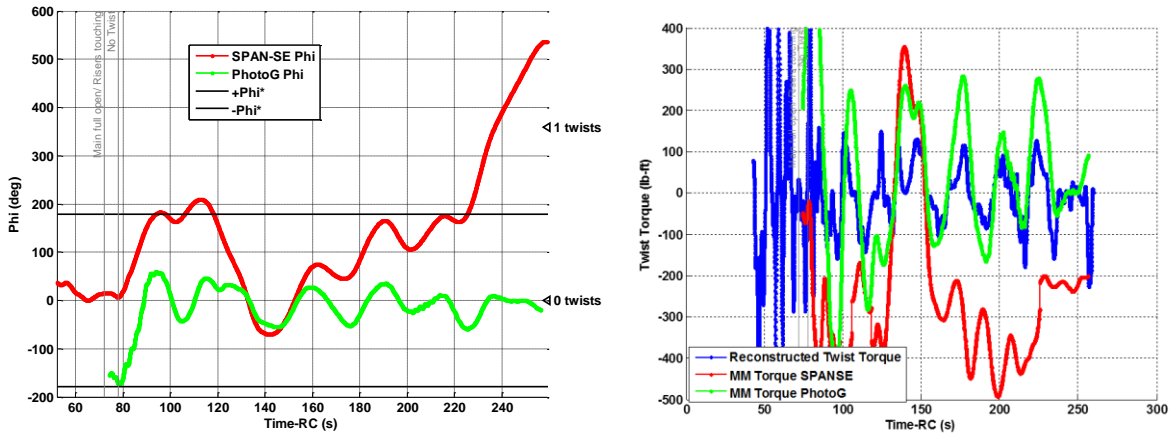


Figure 14. CDT-3-2 Twist Angle and Twist Torque.

C. Phase III: CDT-3-3 and CDT-3-5 PTV Test

The PTV is a truncated capsule that is the closest in similarity to the Orion/Multi Purpose Crew Vehicle. The axis system is also slightly changed between the PCDTV and PTV as shown in Fig. 15. The exact same methodology was used between Phase II and Phase III the only difference being the test vehicles. Due to the change in the axis system the yaw rate had a significant increase in effect on the twist rate as shown in Fig. 16. In Fig. 16 at about T-RC 95 the main steady state phase of flight began. The twist rate and twist angle were also calculated in the same way as in Phase II.

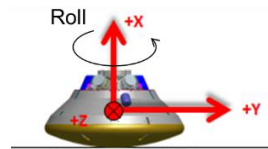


Figure 15. PTV System.

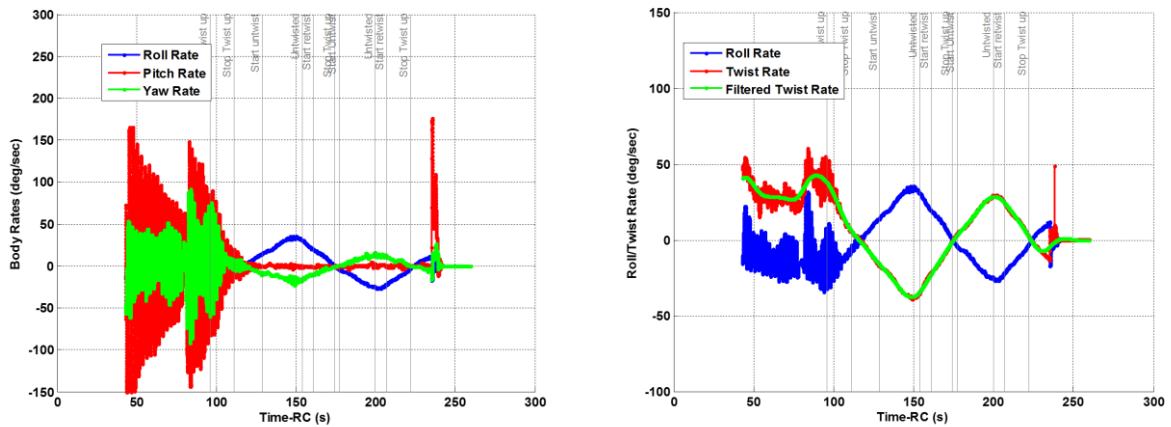


Figure 16. CDT-3-3 Rates.

The simulation was run and twist torque was again calculated for CDT-3-3 and CDT-3-5 as shown in the following figures.

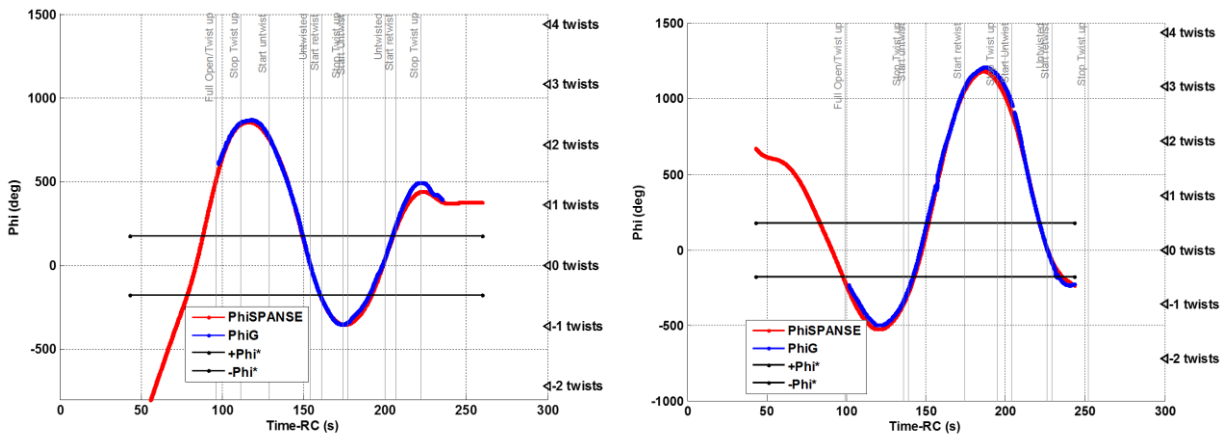


Figure 17. CDT-3-3 and CDT-3-5 (respectively) Twist Angles.

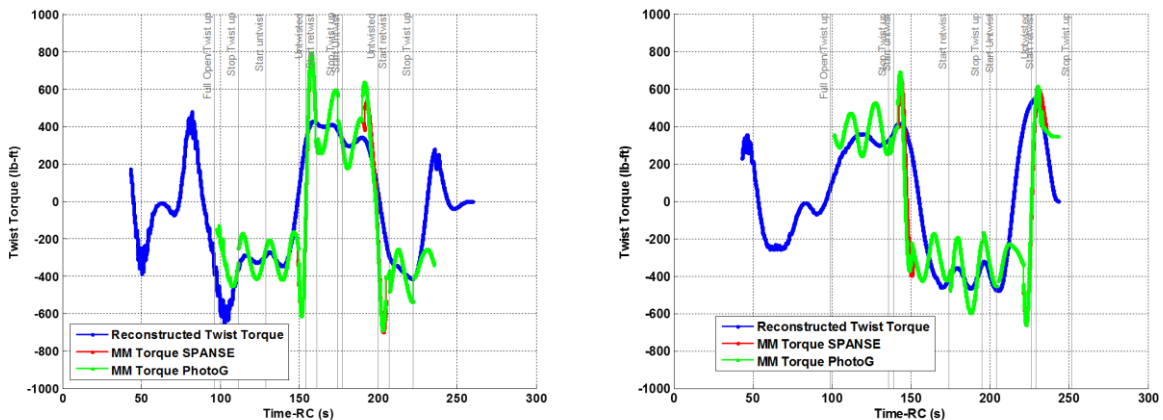


Figure 18. CDT-3-3 and CDT-3-5 (respectively) Twist Torques.

As Fig. 18 shows the Model Memo Torque Equation (green and red traces) was a good match for the true torque (blue trace) and was conservative.

IV. Conclusion

A successful reconstruction of twist torque in Main parachute risers is presented. The Model Memo Conservative Torque Equation for steel risers using photogrammetrics matches test data well. As shown in the twist angle in Fig. 14 photogrammetrics is more reliable due to accounting for relative position of the parachutes to the body. The Model Memo is conservative with respect to the test data, but is acceptable. The Model Memo k and R_w parameters are correct for tests using steel risers, but will need to be re-evaluated for the new textile risers. If a closer match to test data is desired the k parameter would need to be varying based on time and twist position. It is concluded that the Model Memo equations and the simulation can accurately predict Main parachute riser twist torque and should be used in future tests.

Acknowledgments

The author wishes to acknowledge the contributions of Dr. Vladimir Drozd of Airborne Systems North America in deriving the Model Memo equations, Chris Madsen of NASA-JSC in the reconstruction of twist torque of CDT-3-1 and CDT-3-2, and Eric Ray (MRI Technologies) and John Davidson (GeoControl Systems, Inc.) of the JSC Engineering Technology and Science contract (JETS) in the assistance and guidance in the development of the simulation.

References

¹Ray, E. S., *et al.*, *Capsule Parachute Assembly System (CPAS) Engineering Development Unit Operating Modeling Parameters Version 13*, JSC 65914 Rev I, ESCG-8400-CPAS-10-CPAS-MEMO-0069 Rev I, April 2014, JSC Engineering Technology and Science, Jacobs Engineering.